PRONUMERIX

Independent SoundSim360 Analysis of the Proposed Vosnæs Wind Farm

Updated A-Weighted Sound, Indoor Low-Frequency Sound, and Infrasound Propagation
Physics-Based Full-Wave Modelling of the Three-Turbine Layout

Prof. Ken Mattsson
Professor of Scientific Computing, Uppsala University
Chief Executive Officer, Pronumerix AB

October 2026, updated version

Executive Summary

On behalf of the association *Foreningen mod vindmøller ved Vosnæs*, Pronumerix AB has prepared an updated independent assessment of sound propagation from the proposed three-turbine wind farm at Vosnæs, Denmark. This report replaces the numerical results, maps, and result-based conclusions in the previous Vosnæs assessment. The calculations use *SoundSim360*, a physics-based numerical framework for three-dimensional acoustic wave propagation.

The updated assessment considers three distinct acoustic quantities: conventional outdoor A-weighted sound pressure levels; estimated indoor A-weighted low-frequency levels summed over the one-third-octave bands from 10 to 160 Hz; and unweighted sound pressure levels at 1 Hz. The 6 and 8 m/s calculations use the same representative nighttime inversion profile as the previous assessment. A separate 1 Hz calculation uses another atmosphere and one fixed wind direction at 4 m/s.

At the twelve receptor locations A–L, the calculated outdoor A-weighted levels range from 36.3 to 41.4 dBA at 6 m/s and from 36.6 to 41.5 dBA at 8 m/s. Using the receptor classifications carried forward from the previous report, the nominal results at J and K are above the 37 dBA criterion at 6 m/s by 2.1 and 1.3 dB, respectively. At 8 m/s, J is 0.2 dB above the corresponding 39 dBA criterion, while K is 0.4 dB below it. The remaining receptors are below the 42/44 dBA criteria assigned to open-country residential locations. The Havhuse summer-house area contains substantially more dwellings than the two strategic receptors J and K; these two points should therefore not be interpreted as an exhaustive assessment of all individual summer houses. These comparisons are provided as regulatory context; formal compliance is determined under the prescribed Danish assessment procedure.

The estimated indoor low-frequency levels over 10–160 Hz range from 11.9 to 16.2 dBA at 6 m/s and from 12.2 to 16.3 dBA at 8 m/s. All twelve nominal values are below the Danish indoor low-frequency criterion of 20 dBA. This result is specific to the 10–160 Hz metric and the assumed source and building-transmission treatment; it does not characterize infrasonic exposure below 10 Hz.

The separate 1 Hz calculations give unweighted receptor levels of 102.7–106.1 dB at 6 m/s, 102.9–106.1 dB at 8 m/s, and 101.1–105.1 dB in the separate 4 m/s case. All twelve receptors are above 100 dB at 1 Hz in all three calculations. These values are frequency-specific physical exposure estimates, not broadband 1–20 Hz totals and not direct predictions of audibility or health effect.

An important scientific uncertainty concerns long-term exposure to the periodic infrasonic signal generated by modern large wind turbines. The blade-passage frequency (BPF) of modern turbines is typically in the range of approximately 0.2–0.5 Hz, with distinct harmonics at multiples of the BPF. Existing experimental studies do not adequately reproduce long-duration exposure to this very-low-frequency, periodic signal at levels comparable to those assessed here. This evidence gap is discussed explicitly in the report, together with the distinction between absence of demonstrated harm and absence of relevant long-term evidence.

The results should be interpreted as physically based propagation estimates for the specified source and atmospheric scenarios. Source characterization, atmospheric variability, building transmission, ground conditions,

and the exact prescribed regulatory calculation method all remain relevant to the final assessment.

Disclaimer and commissioning statement: This report was commissioned by Foreningen mod vindmøller ved Vosnæs and has been prepared by Pronumerix AB. The modelling methodology, numerical results, and scientific interpretation are those of Pronumerix AB and the author. References to Uppsala University describe the author's academic affiliation and the research background of the methods and do not imply institutional endorsement of the conclusions presented here.

Project Configuration and Input Data

The project configuration considered in this update consists of three **Vestas V136–4.5 MW** wind turbines with a hub height of **82 m**. Turbine positions are carried forward from the EMD International A/S project documents *231215 Vosnæs – 3 x V136 – normal støj* and *231215 Vosnæs – 3 x V136 – lavfrekvent støj*. The twelve receptor locations A–L use the coordinates supplied with the updated SoundSim360 result files. Coordinates are in EPSG:25832 (ETRS89 / UTM zone 32N).

For the conventional outdoor calculation, the A-weighted source-level reference carried forward from the original Vosnæs assessment and EMD documentation is $L_{WA} = 103.9$ dB per turbine. A complete manufacturer one-third-octave spectrum, including operating mode and wind-speed dependence, was not included in the material supplied for the present update and has therefore not been independently verified in this report.

Low-frequency source data for the Vestas V136–4.5 MW are used within the Danish 10–160 Hz assessment framework. For the turbine configuration considered here, the available project documentation reports total A-weighted low-frequency sound-power levels of 91.5 dBA at 6 m/s and 91.8 dBA at 8 m/s. The corresponding one-third-octave source spectrum, however, was not included in the material supplied for the present update. Consequently, while the total low-frequency source levels are known, the bandwise source input used in the calculations cannot be independently verified from the supplied documentation. The updated low-frequency result files contain aggregated indoor 10–160 Hz receptor levels and are therefore reported as SoundSim360 estimates conditional on the underlying spectral and facade-transmission assumptions.

For the infrasound calculations, each turbine is assigned a separate measurement-based source strength of $L_W = 163$ dB at 1 Hz. This value is based on inverse modelling of calibrated field measurements of modern 4.3–6.6 MW turbines at Målarberget and Lervik, Sweden [26]. It is a transfer assumption rather than a manufacturer-certified 1 Hz source value for the Vestas V136–4.5 MW turbine.

The 6 and 8 m/s calculations use the nighttime atmospheric profile from 31 March 2023 at 04:00, which contains a temperature inversion. Downwind propagation is evaluated for the relevant source–receiver directions. These maps should therefore be interpreted as downwind screening scenarios, rather than as one simultaneously realizable wind vector directed toward all receptor locations. The separate 4 m/s calculation uses another atmosphere and a fixed wind direction indicated by the arrow on the supplied map. The exact date, time, and meteorological bearing for this 4 m/s case were not included in the result exports.

The original Vosnæs setup used ordinary ground represented by impedance class E in the Nord2000 ground classification [1], with atmospheric absorption according to ISO 9613-1:1993 [12]. The updated receptor exports provide coordinates, levels, and nearest-turbine distances but do not contain the complete ground map, receptor extraction height, or numerical run settings. The interpretation here consequently carries forward the documented physical setup where those details were not contained in the new exports.

Atmospheric, ground, and source-side variability. The selected nighttime inversion profile represents one adverse propagation state rather than the full range of conditions that may occur at Vosnæs. Changes in wind and temperature gradients can alter refraction and the formation of focusing or shadow regions, while changes in effective ground impedance and the land–water transition can modify interference and attenuation. The present calculations therefore do not define a statistical upper or lower envelope of long-term sound levels, and the magnitude of site-specific variability cannot be quantified from the available input data alone.

The acoustic source is likewise prescribed rather than generated from an aerodynamic rotor model. The V136 rotor spans approximately 14–150 m above ground for an 82 m hub height, so the blades sample a substantial vertical range of the atmospheric boundary layer. Actual sound emission may vary with vertical wind shear, turbulence, yaw conditions, operating state, and wake interaction between turbines. These source-side effects are not explicitly modelled here. Their direction and magnitude should not be assumed a priori, but they constitute an additional uncertainty when transferring manufacturer or project source spectra to a specific operating site.

Table 1: Strategic receptor locations used in the updated Vosnæs assessment. Coordinates are EPSG:25832; distance is to the nearest turbine.

Location	Easting [m]	Northing [m]	Nearest turbine [m]
A	583856.91	6238238.73	858
B	583891.56	6238448.36	850
C	584367.33	6239083.55	914
D	584957.95	6239085.11	881
E	585088.90	6239075.28	917
F	585578.82	6238435.59	886
G	585663.32	6238318.89	952
H	585689.08	6238280.80	975
I	585766.80	6238186.88	1031
J	585235.87	6238738.64	722
K	585485.62	6238707.97	903
L	584095.40	6238289.61	622

High-Fidelity Modelling with SoundSim360

SoundSim360 is a physics-based three-dimensional acoustic propagation framework built on high-order finite-difference methods. It solves the acoustic wave equation directly and can represent terrain, ground impedance, atmospheric refraction, diffraction, reflection, interference, and complex propagation paths in a unified full-wave model. The framework also includes frequency-dependent atmospheric absorption, treated consistently with ISO 9613-1:1993 [12].

The numerical foundation of *SoundSim360* has been developed over more than two decades through a sequence of studies on stable and accurate high-order finite-difference methods, summation-by-parts (SBP) operators, weak boundary and interface treatments, curvilinear multiblock grids, and wave propagation in heterogeneous media [20, 30, 21, 27, 28, 19, 22, 3, 18, 23, 36, 24, 31, 17, 2, 43, 42, 29, 34]. These methods form the numerical basis for large-scale GPU-accelerated full-wave calculations. The formulation, implementation, validation, and application of *SoundSim360* to low-frequency sound and infrasound propagation are described in [26]. The same wave-based framework has recently been applied to road-traffic noise in complex real-world environments containing terrain variations, buildings, and noise barriers, including direct comparison with Nord2000 as implemented in *SoundPLAN 9.1* [25].

Conventional engineering models such as Nord2000 [1] and ISO 9613-2:2024 [13] are useful and widely used for environmental-noise prediction, but they are not direct numerical solutions of the full three-dimensional acoustic wave equation. Their treatments of propagation, diffraction, ground interaction, and atmospheric effects necessarily involve approximations. This distinction becomes increasingly important at low frequencies, in complex terrain, near buildings or barriers, and when multiple propagation paths and strong atmospheric refraction are present.

At low frequencies and in the infrasonic range, wavelengths are large relative to many terrain and built-environment features, and diffraction, reflection, interference, and atmospheric refraction can strongly influence the sound field. Previous work has demonstrated significant differences between simplified propagation models and full-wave solutions in complex terrain [3]. Field studies have also reported situations in which conventional wind-turbine noise calculations underestimate measured A-weighted levels under particular propagation conditions, including stable nighttime conditions at distances of approximately 1 km [15]. These observations motivate the use of a complementary full-wave calculation for the present assessment.

As an illustrative example, Figure 1 compares *SoundSim360* with Nord2000 as implemented in *SoundPLAN 9.1* for a 31.5 Hz source at Polacksbacken, Uppsala University. The comparison shows substantial differences in building-induced shadow regions and illustrates why full-wave modelling becomes important at low frequencies.

For the original Vosnæs documentation, EMD International A/S used the Danish 2019 calculation method in *windPRO 4.0.528*. This is the relevant project-specific engineering calculation for comparison and should not be described as a Nord2000 calculation. The present report contains the updated SoundSim360 results and does not reproduce EMD's earlier maps as current results.

Why Infrasound Is Assessed Separately

A-weighting is designed primarily for conventional audible-noise assessment and strongly attenuates low-frequency components, particularly below approximately 20 Hz. Consequently, an A-weighted result does not describe

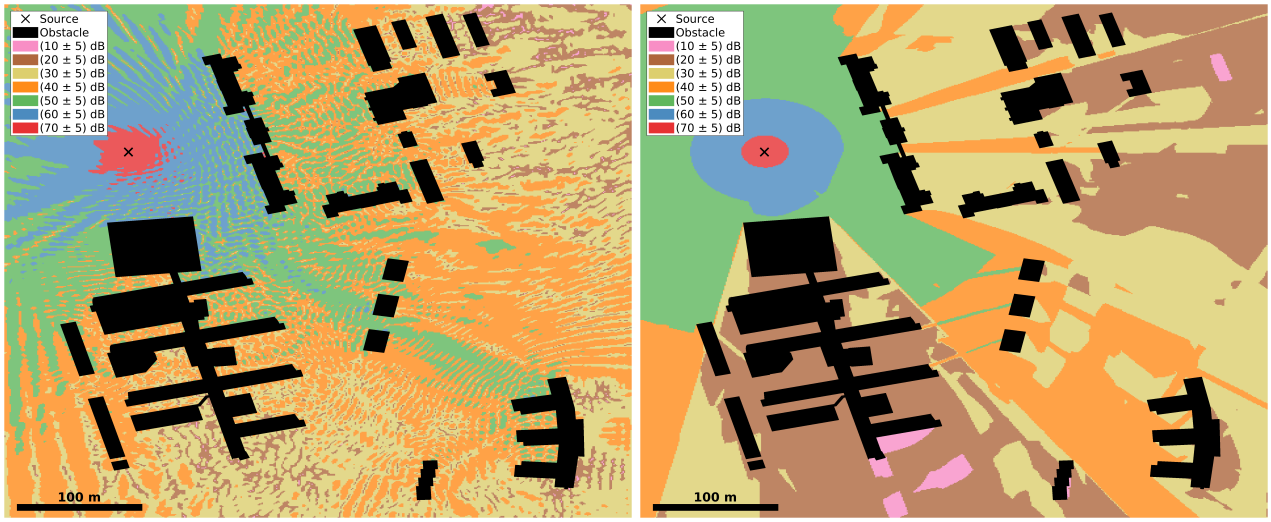

(a) *SoundSim360* (b) *Nord2000*

Figure 1: Low-frequency sound simulation at 31.5 Hz for a 105 dB monopole source located at Polacksbacken, Uppsala University. The source is located 10 m above ground. The panels show sound pressure levels 2 m above ground calculated using (a) *SoundSim360* and (b) Nord2000 as implemented in *SoundPLAN 9.1*.

the unweighted infrasonic pressure field. This is important for large modern wind turbines because the relative contribution of low-frequency sound increases with turbine size, while characteristic rotational frequencies shift toward lower frequencies [32, 41]. Recent measurements of large turbines are consistent with this general trend [46].

The indoor Danish low-frequency metric used in this report covers 10–160 Hz and is also distinct from the infrasonic field below 10 Hz. It cannot be used to infer the sound pressure at 1 Hz or at the blade-passage frequency. Conversely, the 1 Hz calculation is not a substitute for the 10–160 Hz indoor criterion. These quantities describe different parts of the acoustic spectrum and should be reported separately.

The 1 Hz calculations are not obtained by extrapolating the project A-weighted source level or the indoor low-frequency metric. Instead, they use $L_W = 163$ dB at 1 Hz per turbine as a separate measurement-based source assumption. The underlying field measurements were obtained with calibrated instrumentation and were used to validate the propagation model and infer source strength for modern large turbines [26]. The actual 1 Hz source strength of the proposed Vosnæs V136 turbines has not been supplied by the manufacturer and remains an important source uncertainty.

Figure 2 illustrates the difference between unweighted infrasonic sound pressure and conventional frequency-weighted metrics. Measurements during turbine operation and shutdown demonstrate a strong turbine contribution in the 1–20 Hz range at the measured sites, while the A-weighted contribution is much smaller because of the strong low-frequency attenuation introduced by A-weighting [26].

Scientific Context: Low-Frequency Sound, Infrasound, and Exposure

Long-term exposure to environmental noise has been associated with adverse health outcomes, including cardiovascular effects [6, 47]. These findings concern environmental noise in general and should not be interpreted as establishing a direct health effect from the 1 Hz levels calculated in the present study. They do, however, motivate careful characterization of the full acoustic exposure rather than reliance on a single summary metric.

For wind-turbine assessments, A-weighted levels remain important because they are widely used in regulation and environmental-noise practice. At the same time, A-weighting strongly suppresses very-low-frequency and infrasonic sound and therefore provides little information about the unweighted pressure field below approximately 20 Hz. The Danish indoor low-frequency metric used in the present assessment extends from 10 to 160 Hz and consequently also excludes the infrasonic components below 10 Hz. Conventional outdoor dBA, indoor 10–160 Hz dBA, and unweighted infrasound should therefore be regarded as complementary rather than interchangeable acoustic quantities.

The transmission of low-frequency sound into buildings is another relevant issue. Regulatory and engineering assessments often estimate indoor levels by applying tabulated facade-attenuation values to outdoor predic-

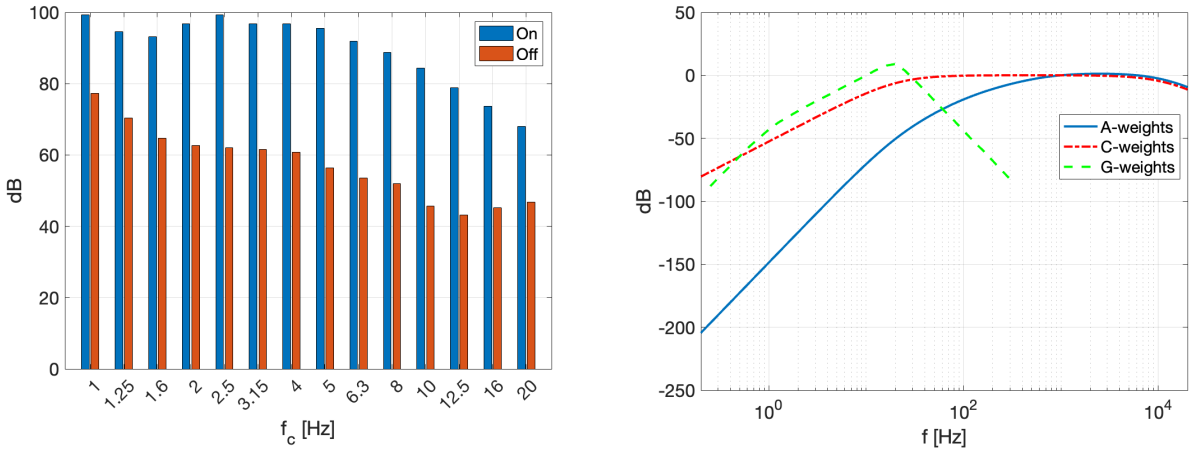

(a) Sound pressure

(b) A-, C-, and G-weighting

Figure 2: (a) Measured infrasound levels during wind-turbine operation and turbine shutdown, demonstrating the turbine contribution to low-frequency and infrasonic sound. (b) Frequency-dependent attenuation introduced by A-, C-, and G-weighting filters.

tions [11]. The general applicability of such simplified attenuation values has been questioned in the acoustic literature [33]. Several field investigations have also reported cases in which indoor infrasonic levels were comparable to, or locally higher than, corresponding outdoor levels because of structural coupling and room-pressure effects [14, 4, 7, 5]. The estimated indoor 10–160 Hz levels presented in this report therefore provide information about the Danish low-frequency metric but should not be interpreted as a prediction of indoor exposure at approximately 1 Hz or below. A building-specific infrasonic assessment would require explicit modelling or measurements at those frequencies.

Human auditory sensitivity decreases steeply in the infrasonic range. The calculated 1 Hz levels should therefore not be interpreted in the same way as conventional audible sound levels, and the present values are expected to be below the threshold of conscious auditory perception at 1 Hz. However, conscious audibility and physiological interaction are not equivalent concepts. Experimental and mechanistic studies have reported cochlear, neural, autonomic, or affective responses to low-frequency sound and infrasound under specific exposure conditions [8, 37, 38, 39, 48, 10, 40].

The exposure conditions in these studies differ substantially from the present 1 Hz calculations and should not be treated as direct dose–response analogues. Weichenberger et al. [48] used a 12 Hz pure tone and defined the near-threshold condition individually at 2 dB below each participant's measured hearing threshold; the median 12 Hz hearing threshold in that experiment was 86.5 dB SPL. Forlim et al. [10] exposed participants to inaudible 6 Hz infrasound at 80–90 dB SPL for 8 hours per night over four weeks and reported changes in resting-state functional connectivity. More recently, Scatterty et al. [40] used approximately 18 Hz exposure at 75–78 dB; participants did not identify the exposure above chance, while differences were reported in salivary cortisol and selected affective measures. Danielsson and Landström [8] studied 6, 12, and 16 Hz exposures at higher linear sound-pressure levels; their study is therefore relevant mainly as evidence that infrasonic exposure can produce physiological responses under sufficiently strong experimental conditions.

None of these studies establishes a dose–response relationship for 1 Hz exposure at the levels predicted at Vosnæs, and none demonstrates that the present calculated levels cause adverse health effects. Their relevance here is narrower: they show that the conscious hearing threshold alone is not a sufficient criterion for declaring an infrasonic exposure biologically irrelevant. The numerical results in this report are therefore treated as physical exposure estimates rather than as direct health-effect predictions.

A particularly important remaining knowledge gap concerns long-term exposure to very-low-frequency infrasound at approximately 1 Hz and below. Modern large wind turbines generate a characteristic periodic infrasonic signal associated with the blade-passage frequency (BPF), typically approximately 0.2–0.5 Hz, together with distinct harmonics at integer multiples of the BPF [26]. Each blade passage generates a pressure pulse, producing a repetitive temporal structure that appears in measured spectra as discrete peaks at the BPF and its harmonics. This differs from much of the naturally occurring atmospheric infrasound, which is predominantly broadband and does not exhibit the same persistent turbine-related harmonic structure.

In the turbine on/off measurements shown in Figure 2, operation of the turbines produces substantially higher infrasonic sound pressure than the turbine-off background over much of the measured frequency range [26].

These measurements were performed at Swedish wind farms and should not be interpreted as measurements at Vosnæs. They nevertheless illustrate an important physical characteristic of modern wind-turbine infrasound: the relevant exposure is not characterized solely by an average sound-pressure level, but also by a persistent periodic and pulsating structure related to turbine rotation.

The available experimental literature does not adequately address chronic exposure to this specific type of signal. Existing studies generally use different frequencies, shorter exposure periods, or stimulus waveforms that do not reproduce the very-low-frequency BPF and harmonic structure characteristic of modern large wind turbines. In particular, long-duration controlled studies have not reproduced realistic periodic turbine-like pressure signals extending down to the fundamental BPF while maintaining exposure over extended periods. The possible consequences of chronic exposure around 1 Hz and below, at levels comparable to those modelled here, therefore remain insufficiently investigated.

This distinction is important when interpreting the present results. The absence of established adverse health effects from long-term exposure at approximately 1 Hz and below should not be interpreted as evidence that such exposure is without biological significance. From a precautionary-principle perspective, the unresolved evidence gap provides a reason to characterize and report the exposure explicitly and to support further long-duration studies using realistic turbine-like pressure waveforms, including the BPF and its harmonics. Application of the precautionary principle in this context does not imply that adverse health effects have been demonstrated; rather, it acknowledges that the exposure scenario characteristic of modern large wind turbines has not yet been adequately investigated.

The literature consequently remains incomplete with respect to mechanisms, exposure–response relationships, individual susceptibility, and long-term effects. Broader research on environmental sensitivity also indicates substantial inter-individual differences in sensory responsiveness [16, 35]; these studies are not specific to infrasound and are cited here only in relation to variability between individuals.

Potential effects on wildlife. Potential effects of wind-power development on wildlife are also relevant in environmental assessment. A growing body of field research indicates that wind-power developments can alter habitat use, migration, and movement patterns of terrestrial mammals over distances considerably larger than the immediate turbine footprint. A systematic review by Tolvanen et al. [45] found displacement in all six cases involving semi-domesticated reindeer. Reported responses extended over several kilometres, with individual studies documenting effects at distances of up to approximately 15 km from wind-power developments. This should not be interpreted as a universal exclusion distance, since the magnitude and spatial extent of the response varied between studies, seasons, habitats, and phases of wind-farm development.

Eftestøl et al. [9] followed semi-domesticated reindeer in the Rákkonjárga district in Finnmark, Norway, before, during, and after construction of the Rákkočearru wind farm. Up to 36 GPS-collared females were monitored annually over the 2011–2019 study period, and habitat use was analysed at both landscape and individual home-range scales. The study documented changes in habitat use over several kilometres and, in some seasons and spatial analyses, over distances of approximately 10 km or more. During spring, habitat use was approximately 32–35% lower within a zone extending roughly 2–13 km from the wind farm during and after development compared with the pre-development period. In autumn, the authors reported a 72% reduction in use extending up to approximately 15 km during construction and a 38% reduction extending up to approximately 12 km after construction. At the individual home-range scale, reduced use was also reported over several kilometres, including approximately 3–11 km during spring and up to about 6 km during summer.

These findings illustrate that the spatial extent of reported behavioural responses to wind-power development can extend much farther than the immediate turbine footprint. However, the authors emphasized that the magnitude and even direction of the response depended on season, spatial scale, annual conditions, and herding activity. The evidence therefore does not support a single fixed exclusion distance applicable to all wind farms or species.

Importantly, these ecological studies concern the combined presence of wind-power infrastructure and associated disturbance and do not establish acoustic exposure, or infrasound specifically, as the causal mechanism. Visual exposure, rotor movement, roads, human activity, habitat fragmentation, altered migration routes, and acoustic disturbance may all contribute. Possible effects of infrasonic acoustic energy on navigation cues have also been discussed for birds and cetaceans [44]; this does not establish a corresponding mechanism in terrestrial mammals or other wildlife around Vosnæs.

The present SoundSim360 calculations therefore cannot by themselves predict ecological effects around the Vosnæs project. They do, however, provide a physics-based description of acoustic exposure that may extend well beyond the immediate turbine locations. A useful research direction would be to combine animal GPS trajectories or other ecological observations with meteorological data and physics-based acoustic modelling. This would allow time-dependent acoustic exposure to be tested against distance, visibility, habitat, human activity,

and other competing explanatory variables rather than using distance to the nearest turbine alone.

Wind-turbine sound can also exhibit amplitude modulation at audible frequencies, particularly under certain atmospheric and operational conditions [15]. Such temporal characteristics are not fully represented by a stationary long-term A-weighted metric. The present calculations describe propagation under specified source and atmospheric scenarios and do not explicitly model time-varying amplitude modulation. The A-weighted maps should therefore not be interpreted as predictions of modulation depth, short-term peak-to-trough variation, or the occurrence frequency of AM at individual dwellings.

A-Weighted Sound Propagation

The conventional outdoor assessment uses the source-level reference $L_{WA} = 103.9$ dB per turbine and the three-turbine layout described above. The 6 and 8 m/s cases use the nighttime inversion profile from 31 March 2023 at 04:00. The updated maps are shown in Figure 3.

Across the twelve receptor locations, calculated outdoor levels range from 36.3 to 41.4 dBA at 6 m/s and from 36.6 to 41.5 dBA at 8 m/s. The largest value occurs at receptor L, 622 m from the nearest turbine.

Regulatory context. Danish wind-turbine criteria are 42/44 dBA at 6/8 m/s for outdoor residential areas in open country and 37/39 dBA in areas designated for noise-sensitive land use. The receptor classifications used here follow the previous Vosnæs report: J and K are compared with the stricter 37/39 dBA criteria, while A–I and L are compared with 42/44 dBA. The nominal results at J and K are 39.1 and 38.3 dBA at 6 m/s, respectively, and 39.2 and 38.6 dBA at 8 m/s. Thus, the SoundSim360 values are nominally above the assigned criteria at J and K at 6 m/s and at J at 8 m/s. The remaining receptor values are below the criteria assigned to them. These comparisons are provided as regulatory context only. Formal compliance is determined using the prescribed Danish calculation procedure, receptor classification, averaging conventions, and applicable corrections.[1]

Representativeness of J and K for Havhuse. J and K are strategic receptor locations within the Havhuse summer-house area, but they do not represent a house-by-house assessment of the wider area. According to information supplied by the commissioning group, approximately 81 summer houses are located in the area subject to the 37/39 dBA criteria. The spatial contours in Figure 3 indicate that the predicted field varies across this area. Consequently, the values at J and K cannot by themselves establish the regulatory status of every dwelling. A formal assessment of Havhuse should evaluate the relevant individual dwellings, or otherwise demonstrate that the selected receptors capture the most exposed locations.

Indoor Low-Frequency Sound Propagation

The updated low-frequency results are estimated indoor A-weighted levels summed over the one-third-octave bands from 10 to 160 Hz. They use the same nighttime inversion profile and 6/8 m/s downwind scenarios as the outdoor A-weighted calculations. The indoor metric is separate from both the outdoor full-spectrum dBA level and the unweighted infrasonic field below 10 Hz.

At 6 m/s, the estimated indoor levels range from 11.9 dBA at E to 16.2 dBA at L. At 8 m/s, they range from 12.2 dBA at E to 16.3 dBA at L. All twelve nominal results are below the Danish indoor low-frequency criterion of 20 dBA at both wind speeds. The minimum nominal margin is 3.8 dB at 6 m/s and 3.7 dB at 8 m/s, both at receptor L.

The result is conditional on the assumed source spectrum and outdoor-to-indoor transmission treatment. The exported results do not provide the complete bandwise source spectrum or dwelling-specific facade properties, and the maps do not resolve sound fields inside individual buildings. In particular, the transmission treatment has not been validated against the local building stock. Many of the Havhuse dwellings are reported to be lightweight timber summer houses, for which the frequency-dependent facade transmission may differ from generic or tabulated attenuation values. The present indoor values should therefore not be interpreted as dwelling-specific predictions.

The missing one-third-octave source spectrum is also a material uncertainty. Two source spectra with the same total A-weighted level over 10–160 Hz can produce different indoor totals because both outdoor propagation and facade attenuation are strongly frequency dependent. The sensitivity of the reported 10–160 Hz indoor levels to this spectral distribution cannot be quantified reliably without the actual bandwise source data. In

[1] BEK nr 995 af 26/08/2024; Miljøstyrelsen: Vindmøller.

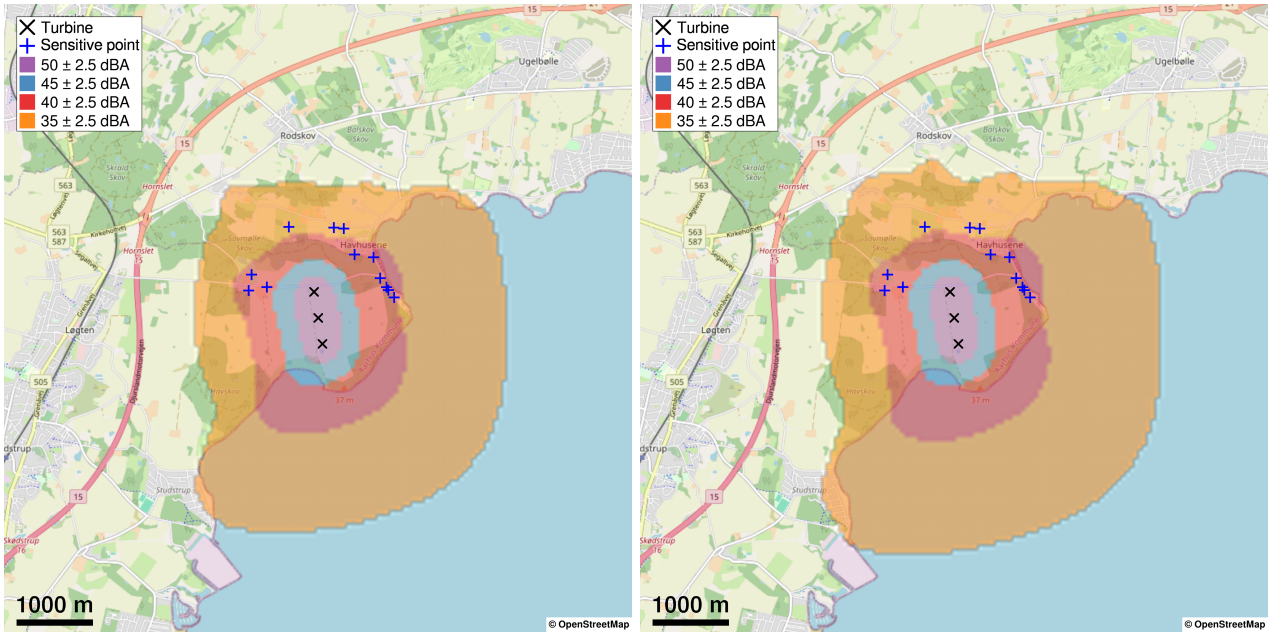

(a) 6 m/s downwind (b) 8 m/s downwind

Figure 3: Updated outdoor A-weighted sound pressure levels at Vosnæs under the nighttime inversion profile. Black crosses mark turbines and blue plus signs mark receptors. The supplied maps use level classes centred on 35, 40, 45, and 50 dBA with half-widths of 2.5 dB. These contour bins are not statistical confidence intervals and do not represent the exact Danish regulatory boundaries.

particular, the nominal 3.7–3.8 dB margin to the 20 dBA criterion at the most exposed receptor should not be interpreted as a validated uncertainty margin. The 10–160 Hz result must also not be extrapolated to 1 Hz or to frequencies below the assessed band.

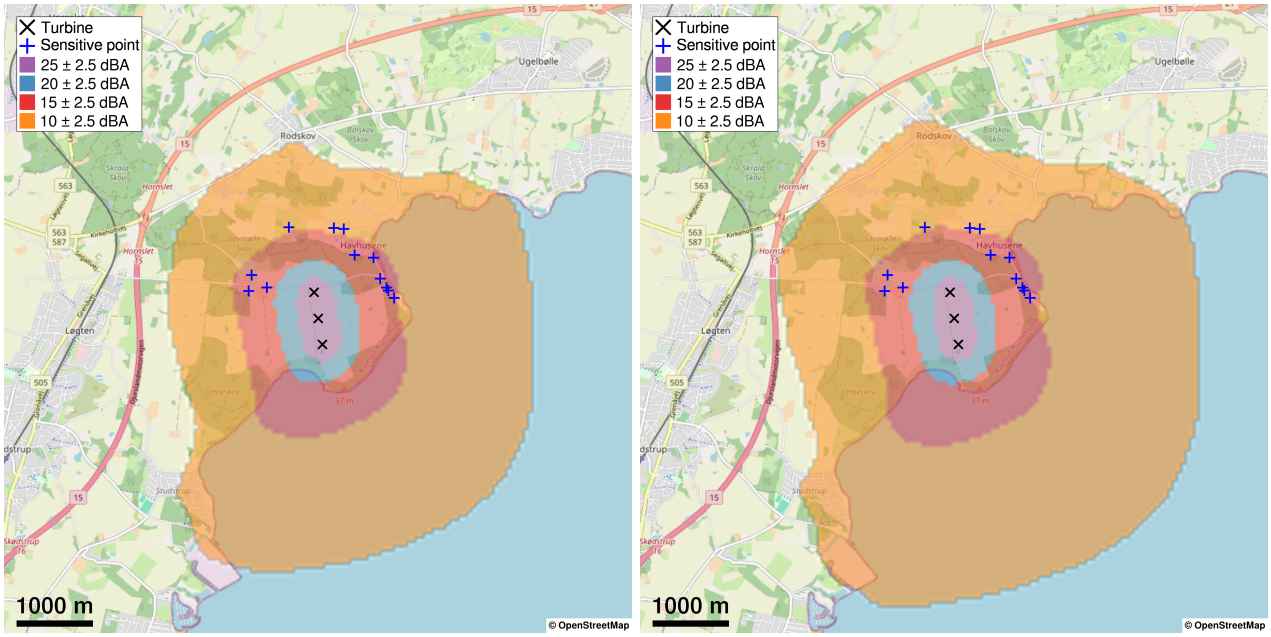

(a) 6 m/s downwind (b) 8 m/s downwind

Figure 4: Updated estimated indoor A-weighted low-frequency levels, summed over 10–160 Hz, under the nighttime inversion profile. The maps are spatial estimates using the assumed indoor transmission treatment; they do not resolve the interiors of individual houses. Level classes are centred on 10, 15, 20, and 25 dBA with half-widths of 2.5 dB.

Infrasound Propagation at 1 Hz

Nighttime 6 and 8 m/s downwind scenarios

For the two nighttime infrasound scenarios, each turbine is assigned the measurement-based source level $L_W = 163$ dB at 1 Hz. The same nighttime inversion atmosphere is used as in the A-weighted calculations. The resulting maps are shown in Figure 5.

At 6 m/s, predicted 1 Hz levels at the twelve receptors range from 102.7 to 106.1 dB. At 8 m/s, the range is 102.9–106.1 dB. All twelve receptors are above 100 dB in both calculations, and the maximum occurs at receptor L. The small differences between the 6 and 8 m/s receptor values apply only to these two specified atmospheric scenarios and should not be interpreted as evidence that infrasound propagation is generally insensitive to meteorology.

These values are unweighted sound-pressure levels at 1 Hz and should not be interpreted as conventional audible dBA levels. They are expected to be below conscious auditory perception at 1 Hz, but this does not itself establish biological irrelevance. The report therefore treats them as physical exposure estimates rather than direct indicators of health effect.

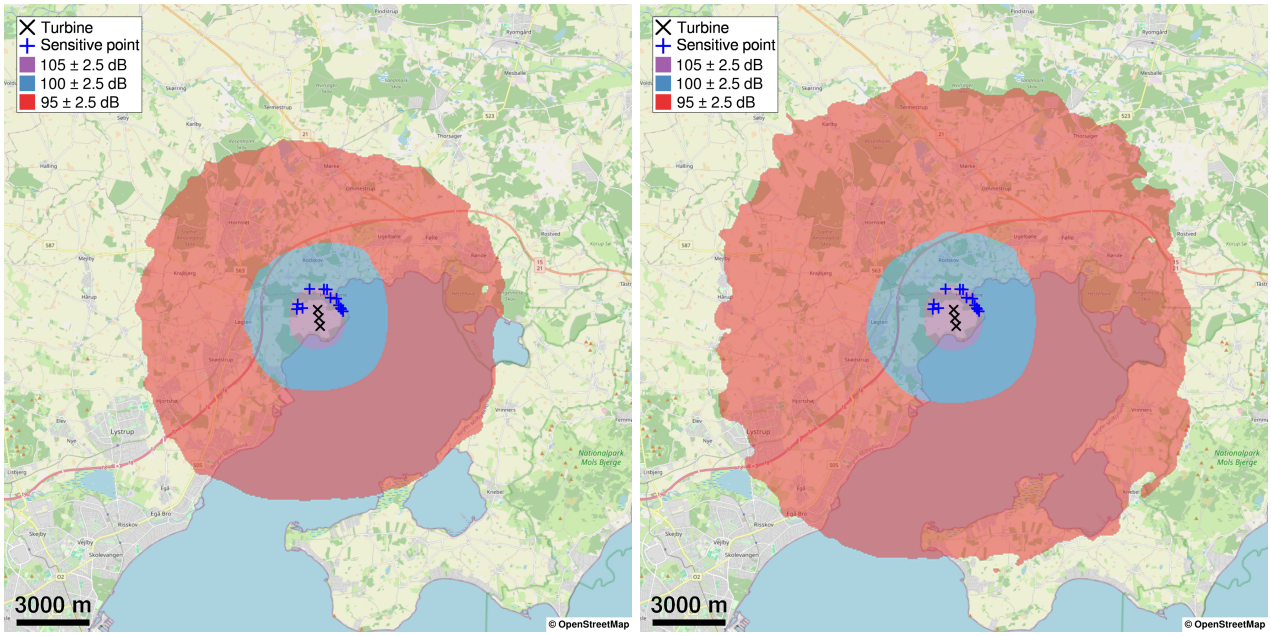

(a) 6 m/s downwind (b) 8 m/s downwind

Figure 5: Updated unweighted 1 Hz sound pressure levels under nighttime inversion conditions. The maps use classes centred on 95, 100, and 105 dB with half-widths of 2.5 dB. The colours denote acoustic levels and should not be interpreted as health-effect thresholds.

Separate atmosphere with directional wind at 4 m/s

A separate 1 Hz calculation uses another atmosphere and one fixed wind direction, indicated by the arrow in Figure 6. The exact date, time, and meteorological bearing of this profile were not included in the updated result files and are therefore not assigned here.

Predicted receptor levels range from 101.1 to 105.1 dB, with the maximum again at receptor L. Relative to the nighttime 6 m/s case, values are 1.0–1.6 dB lower; relative to the nighttime 8 m/s case, they are 1.0–1.8 dB lower. Because both the atmospheric profile and the wind specification differ, these differences cannot be attributed to wind speed alone. The comparison illustrates that atmospheric structure and wind direction modify the spatial distribution and long-range reach of the infrasonic field.

Results at the Strategic Receptor Points

Table 2 summarises all updated receptor values. The A-weighted columns give outdoor full-spectrum levels, the LF columns give estimated indoor A-weighted levels over 10–160 Hz, and the final three columns give

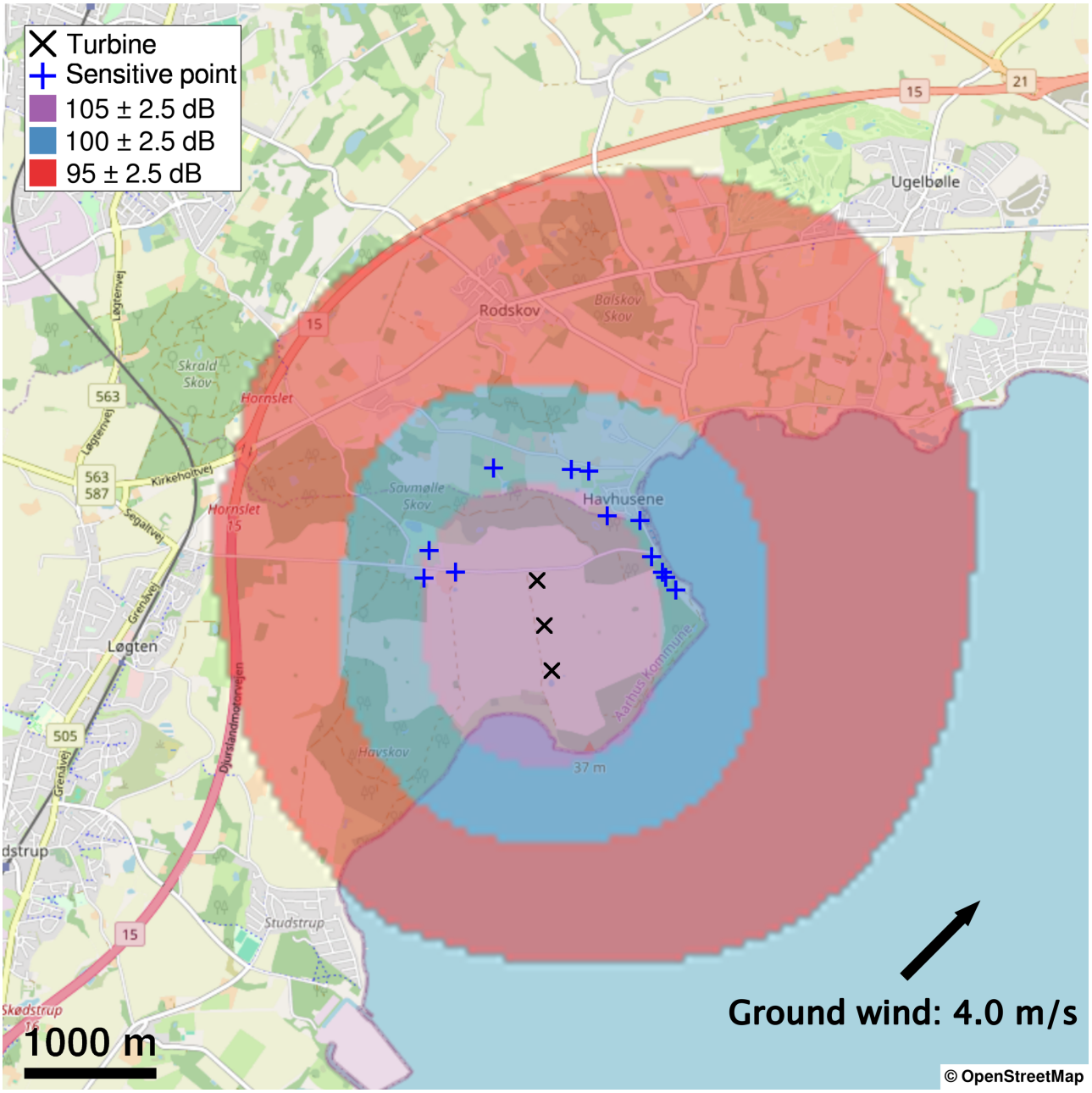

Figure 6: Updated unweighted 1 Hz sound pressure levels using a separate atmosphere and directional wind at 4 m/s. The arrow shows the prescribed wind direction. The map uses the same 95/100/105 dB contour classes and 2.5 dB half-widths as Figure 5; the geographic map scale differs.

unweighted sound-pressure levels at 1 Hz. These quantities must not be combined directly because they use different frequency ranges and, for the low-frequency metric, a different receiving environment.

Table 2: Updated SoundSim360 results at receptors A–L. Outdoor A-weighted levels are shown for 6 and 8 m/s; LF values are estimated indoor A-weighted levels over 10–160 Hz; the final three columns are unweighted 1 Hz levels.

	Outdoor [dBA]		Indoor LF [dBA]		1 Hz [dB]		
Loc.	6 m/s	8 m/s	6 m/s	8 m/s	6 m/s	8 m/s	4 m/s
A	39.6	39.8	14.4	14.6	104.3	104.4	102.8
B	39.0	39.3	14.1	14.3	104.0	104.2	102.5
C	36.7	37.0	12.1	12.3	102.7	102.9	101.1
D	36.3	36.6	12.0	12.3	102.8	103.0	101.3
E	36.4	36.6	11.9	12.2	102.7	102.9	101.1
F	38.8	39.0	13.6	13.8	103.5	103.7	102.3
G	38.5	38.7	13.3	13.5	103.3	103.5	102.0
H	38.4	38.6	13.2	13.4	103.2	103.4	101.9
I	38.0	38.2	12.8	13.1	102.9	103.1	101.5
J	39.1	39.2	14.2	14.3	104.3	104.4	103.1
K	38.3	38.6	13.2	13.4	103.1	103.3	101.8
L	41.4	41.5	16.2	16.3	106.1	106.1	105.1

The reported values retain the one-decimal precision of the supplied exports. This numerical reporting resolution should not be interpreted as a total modelling uncertainty of 0.1 dB. Likewise, the ±2.5 dB values shown in map legends denote contour-bin widths and are not validated confidence intervals for individual receptor predictions.

Interpretation and Limitations

The outdoor dBA, indoor 10–160 Hz dBA, and unweighted 1 Hz results represent distinct acoustic quantities and should not be combined directly. The outdoor calculation uses the project A-weighted source assumptions; the indoor low-frequency calculation additionally depends on spectral and building-transmission assumptions; and the 1 Hz calculation uses a separate measurement-based source strength because no manufacturer-certified V136 source value at 1 Hz was supplied.

The 6 and 8 m/s maps are downwind screening scenarios intended to represent adverse propagation toward the relevant source–receiver directions. They should not be interpreted as one instantaneous wind vector directed toward all receptors at once. The 4 m/s case uses a different atmosphere and a fixed wind direction. Its lower receptor values therefore reflect the combined change in atmospheric structure and wind specification rather than wind speed alone.

Additional uncertainty arises from source characterization, turbine operating mode, atmospheric variability, ground impedance, terrain and land/water representation, receptor height, and building transmission. The complete manufacturer band spectra underlying the current A-weighted and indoor low-frequency results were not supplied with the new exports. This limits independent verification of the spectral inputs. The calculations also do not model changes in acoustic emission caused by wind shear, turbulence, wake interaction, or other aeroacoustic source-side effects, and they do not predict time-varying amplitude modulation.

In particular, the $L_W = 163$ dB source strength used at 1 Hz is transferred from independent measurements of other modern large turbines and should not be confused with a turbine-specific certification value for the Vestas V136–4.5 MW. A direct update should be made if manufacturer-specific unweighted source data at and below 1 Hz become available.

No site-specific background infrasound measurements from Vosnæs were available for this assessment. Natural and anthropogenic infrasonic background varies strongly with frequency, bandwidth, wind, weather, and local activity. The calculated turbine contribution should therefore not be compared directly with a generic background level. A defensible source-versus-background comparison would require measurements at Vosnæs using the same frequency bands and compatible processing, ideally including simultaneous indoor/outdoor measurements and turbine shutdown periods.

A reported level at 1 Hz does not determine the total broadband level over 1–20 Hz, and the present results do not quantify the BPF region below 1 Hz. A broadband infrasonic total requires an explicit spectrum and compatible integration across the relevant frequency bands. Likewise, duration, periodicity, indoor transmission, and occurrence frequency require additional characterization before the calculated 1 Hz levels can be related to long-term personal exposure.

The report does not make a formal legal determination of compliance under Danish wind-turbine noise regulation. Such a determination requires the prescribed Danish calculation method, confirmed receptor classification, the specified averaging and wind-speed conventions, and any applicable corrections. The SoundSim360 calculations provide an independent physics-based comparison and additional information on low-frequency and infrasonic

Table 3: Transparency summary of important inputs, assumptions, and information not available for independent verification in the present update.

Item	Basis used in this report	Status / limitation
Turbine type and layout	Vestas V136–4.5 MW, 82 m hub height; project coordinates	Available from project documentation
Overall outdoor source level	$L_{WA} = 103.9$ dB per turbine	Available; complete manufacturer one-third-octave spectrum not supplied
Low-frequency source level	91.5/91.8 dBA over 10–160 Hz at 6/8 m/s	Total values available; bandwise source spectrum not supplied
1 Hz source strength	$L_W = 163$ dB per turbine from independent field measurements and inverse modelling	Transfer assumption; not a V136 manufacturer-certified value
Atmosphere, 6/8 m/s	Nighttime inversion profile from 31 March 2023 at 04:00	One representative adverse state; not a statistical variability envelope
Atmosphere, 4 m/s	Separate supplied atmosphere and fixed wind direction	Exact date, time, and meteorological bearing not available in the export
Ground treatment	Nord2000 class E carried forward from the original setup	Complete updated ground map not supplied
Indoor transmission	Assumed outdoor-to-indoor transmission treatment	Dwelling-specific facade properties not supplied or validated for Havhuse timber houses
Receptors	Twelve strategic locations A–L	Not an exhaustive house-by-house assessment of the Havhuse summer-house area
Source variability and AM	Prescribed stationary source spectra	Wind shear, turbulence, wake-related source changes, and time-varying AM are not explicitly modelled

propagation.

Conclusions

For the analysed three-turbine Vosnæs layout, the updated SoundSim360 calculations quantify outdoor A-weighted sound, estimated indoor low-frequency sound over 10–160 Hz, and unweighted 1 Hz sound at the twelve receptor locations under the modelled propagation conditions.

For outdoor A-weighted sound, the nominal SoundSim360 results are above the stricter criteria assigned to receptors J and K at 6 m/s and at J at 8 m/s. The corresponding values are 39.1 and 38.3 dBA at 6 m/s and 39.2 and 38.6 dBA at 8 m/s. J and K are strategic locations rather than an exhaustive assessment of the approximately 81 summer houses reported within the Havhuse area, so the status of all individual dwellings cannot be inferred from these two receptor values alone. The remaining receptor values are below the open-country criteria assigned in the previous assessment. These comparisons provide regulatory context but are not themselves a formal Danish compliance determination.

For estimated indoor low-frequency sound over 10–160 Hz, all twelve nominal receptor values are below 20 dBA at both wind speeds. The maximum is 16.3 dBA at receptor L in the 8 m/s case. This result is conditional on both the unavailable bandwise source spectrum and the outdoor-to-indoor transmission assumptions. The latter have not been validated for the lightweight timber summer houses reported at Havhuse. The nominal margin to 20 dBA should therefore not be interpreted as a validated uncertainty margin, and the calculation provides no assessment of frequencies below 10 Hz.

For unweighted infrasound at 1 Hz, all twelve receptors are above 100 dB in each of the three calculations. The nighttime downwind cases reach 106.1 dB at receptor L, while the separate directional 4 m/s case reaches 105.1 dB. These levels are physical exposure estimates, not conventional audible sound levels and not direct health-risk estimates.

The scientific literature does not currently provide an adequate long-term evidence base for chronic exposure to the characteristic periodic BPF-dominated infrasonic signal of modern large wind turbines around 1 Hz and below. This uncertainty does not demonstrate adverse health effects, but it also means that absence of established effects should not be treated as evidence that the relevant long-term exposure is biologically insignificant. From a precautionary-principle perspective, the appropriate response is to characterize the exposure transparently and to obtain better long-term data rather than infer safety or harm from the present evidence gap.

For a future project stage, independent long-term measurements at Vosnæs would provide the most direct test of the simulations. Such measurements should include calibrated indoor and outdoor infrasonic sensors, meteorological data, turbine operating information, and preferably planned or naturally occurring turbine shutdown periods. Measurements extending below 1 Hz would be particularly valuable for resolving the BPF and its harmonics. If complete manufacturer source spectra and operating-mode data become available, the calculations should also be updated using those turbine-specific inputs. A more complete regulatory screening of Havhuse should additionally evaluate the individual summer houses and, for indoor low-frequency sound, use measured or otherwise documented transmission data for representative local building constructions.

References

[1] Nina Aguilera, Henrik Naglitsch, and Katrin Olofsson. Beräkningsmanual Nord2000: för bullerberäkningar i väg- och järnvägsplaner. Technical Report 2024:033, Trafikverket, 2024.

[2] Martin Almquist and Eric M. Dunham. Non-stiff boundary and interface penalties for narrow-stencil finite difference approximations of the laplacian on curvilinear multiblock grids. *Journal of Computational Physics*, 408:109294, 2020.

[3] Martin Almquist, Ilkka Karasalo, and Ken Mattsson. Atmospheric sound propagation over large-scale irregular terrain. *Journal of Scientific Computing*, 61(2):369–397, 2014.

[4] Stephen E. Ambrose, Robert W. Rand, and Carmen M. E. Krogh. Wind turbine acoustic investigation: Infrasound and low-frequency noise – a case study. *Bulletin of Science, Technology & Society*, 32(2):128–141, 2012.

[5] Walker B, Hessler G, Hessler D, Rand R, and Schomer P. *A Cooperative Measurement Survey and Analysis of Low Frequency and Infrasound at the Shirley Wind Farm in Brown County, Wisconsin*. Report number 122412-1, 2012.

[6] Mathias Basner, Wolfgang Babisch, Adrian Davis, Mark Brink, Charlotte Clark, Sabine Janssen, and Stephen Stansfeld. Auditory and non-auditory effects of noise on health. *The Lancet*, 383(9925):1325–1332, 2014.

[7] Richard A. Carman. Measurement procedure for wind turbine infrasound. In *INTER-NOISE and NOISE-CON Congress and Conference Proceedings*, volume 250, pages 6143–6153. Institute of Noise Control Engineering, 2015.

[8] Åke Danielsson and Ulf Landström. Blood pressure changes in man during infrasonic exposure. *Acta Medica Scandinavica*, 217(5):531–535, 1985.

[9] Sindre Eftestøl, Diress Tsegaye, Kjetil Flydal, and Jonathan E. Colman. Effects of wind power development on reindeer: Global positioning system monitoring and herders' experience. *Rangeland Ecology & Management*, 87:55–68, 2023.

[10] Caroline Garcia Forlim, Leonie Ascone, Christian Koch, and Simone Kühn. Resting state network changes induced by experimental inaudible infrasound exposure and associations with self-reported noise sensitivity and annoyance. *Scientific Reports*, 14(1):24555, 2024.

[11] Dan Hoffmeyer and Jørgen Jakobsen. Sound insulation of dwellings at low frequencies. *Journal of Low Frequency Noise, Vibration and Active Control*, 29(1):15–23, 2010.

[12] International Organization for Standardization. ISO 9613-1:1993, Acoustics — Attenuation of sound during propagation outdoors — Part 1: Calculation of the absorption of sound by the atmosphere, 1993. International Standard, Edition 1.

[13] International Organization for Standardization. ISO 9613-2:2024, Acoustics — Attenuation of sound during propagation outdoors — Part 2: Engineering method for the prediction of sound pressure levels outdoors, 2024. International Standard, Edition 2.

[14] N D Kelley, H E McKenna, R R Hemphill, C L Etter, R L Garrelts, and N C Linn. Acoustic noise associated with the mod-1 wind turbine: its source, impact, and control. Technical report, Solar Energy Research Inst. (SERI), Golden, CO (United States), 02 1985.

[15] Conny Larsson. Ljud från vindkraftverk, modell-validering-mätning : Slutrapport Energimyndighetens projekt 32437-1. Technical report, Uppsala University, LUVAL, 2014.

[16] Francesca Lionetti, Arthur Aron, Elaine N. Aron, G. Leonard Burns, Jadzia Jagiellowicz, and Michael Pluess. Dandelions, tulips and orchids: evidence for the existence of low-sensitive, medium-sensitive and high-sensitive individuals. *Translational Psychiatry*, 8(1):24, 2018.

[17] Lukas Lundgren and Ken Mattsson. An efficient finite difference method for the shallow water equations. *Journal of Computational Physics*, 422:109784, 2020.

[18] K. Mattsson, M. Almquist, and M. H. Carpenter. Optimal diagonal-norm SBP operators. *Journal of Computational Physics*, 264:91–111, 2014.

[19] K. Mattsson and M. H. Carpenter. Stable and accurate interpolation operators for high-order multi-block finite-difference methods. *SIAM J. Sci Comput.*, 32(4):2298–2320, 2010.

[20] K. Mattsson, M. Svärd, M.H. Carpenter, and J. Nordström. High-order accurate computations for unsteady aerodynamics. *Computers & Fluids*, 36:636–649, 2006.

[21] K. Mattsson, M. Svärd, and M. Shoeybi. Stable and accurate schemes for the compressible navier-stokes equations. *Journal of Computational Physics*, 227(4):2293–2316, 2008.

[22] Ken Mattsson. Summation by parts operators for finite difference approximations of second-derivatives with variable coefficients. *Journal of Scientific Computing*, 51:650–682, 2012.

[23] Ken Mattsson. Diagonal-norm upwind SBP operators. *Journal of Computational Physics*, 335:283 – 310, 2017.

[24] Ken Mattsson, Martin Almquist, and Edwin van der Weide. Boundary optimized diagonal-norm SBP operators. *Journal of Computational Physics*, 2018.

[25] Ken Mattsson and Gustav Eriksson. High-fidelity wave-based simulation of road traffic noise in complex environments. *Applied Acoustics*, 257:111560, 2027.

[26] Ken Mattsson, Gustav Eriksson, Leif Persson, José Chilo, and Kourosh Tatar. Efficient finite difference modeling of infrasound propagation in realistic 3D domains: Validation with wind turbine measurements. *Applied Acoustics*, 243:111156, 2026.

[27] Ken Mattsson, Frank Ham, and Gianluca Iaccarino. Stable and accurate wave-propagation in discontinuous media. *Journal of Computational Physics*, 227(19):8753–8767, 2008.

[28] Ken Mattsson, Frank Ham, and Gianluca Iaccarino. Stable boundary treatment for the wave equation on second-order form. *Journal of Scientific Computing*, 41(3):366–383, 2009.

[29] Ken Mattsson and Ylva Ljungberg Rydin. Implicit summation by parts operators for finite difference approximations of first and second derivatives. *Journal of Computational Physics*, 473:111743, 2023.

[30] Ken Mattsson and Jan Nordström. High order finite difference methods for wave propagation in discontinuous media. *Journal of Computational Physics*, 220(1):249–269, 2006.

[31] Ken Mattsson and Pelle Olsson. An improved projection method. *Journal of Computational Physics*, 372:349 – 372, 2018.

[32] Henrik Møller and Christian Sejer Pedersen. Low-frequency noise from large wind turbines. *The Journal of the Acoustical Society of America*, 129(6):3727–3744, 2011.

[33] Henrik Møller, Steffen Pedersen, Kerstin Persson Waye, and Christian Sejer Pedersen. Comments to the article "sound insulation of dwellings at low frequencies" i. *Journal of Low Frequency Noise, Vibration and Active Control*, 30(3):229–231, 2011.

[34] Pelle Olsson, Gustav Eriksson, and Ken Mattsson. Projection based summation-by-parts methods, embeddings and the pseudoinverse. *Journal of Computational Physics*, 524:113689, 2025.

[35] Michael Pluess, Elham Assary, Francesca Lionetti, Kathryn J. Lester, Eva Krapohl, Elaine N. Aron, and Arthur Aron. Environmental sensitivity in children: Development of the highly sensitive child scale and identification of sensitivity groups. *Developmental Psychology*, 54(1):51–70, 2018.

[36] Ylva Rydin, Ken Mattsson, and Jonatan Werpers. High-fidelity sound propagation in a varying 3D atmosphere. *Journal of Scientific Computing*, 77(2):1278–1302, 2018.

[37] Alec N. Salt and Timothy E. Hullar. Responses of the ear to low frequency sounds, infrasound and wind turbines. *Hearing Research*, 268(1):12–21, 2010.

[38] Alec N. Salt and James A. Kaltenbach. Infrasound from wind turbines could affect humans. *Bulletin of Science, Technology & Society*, 31(4):296–302, 2011.

[39] Alec N Salt and Jeffery T Lichtenhan. How does wind turbine noise affect people. *Acoustics Today*, 10(1):20–28, 2014.

[40] Kale R. Scatterty, Dawson VonStein, Lisa B. Prichard, Brian C. Franczak, Trevor J. Hamilton, and Rodney M. Schmaltz. Infrasound exposure is linked to aversive responding, negative appraisal, and elevated salivary cortisol in humans. *Frontiers in Behavioral Neuroscience*, 20:1729876, 2026.

[41] Bo Søndergaard. Low frequency noise from wind turbines: Do the danish regulations have any impact? an analysis of noise measurements. *International Journal of Aeroacoustics*, 14(5-6):909–915, 2015.

[42] Vidar Stiernström, Martin Almquist, and Ken Mattsson. Boundary-optimized summation-by-parts operators for finite difference approximations of second derivatives with variable coefficients. *Journal of Computational Physics*, 491:112376, 2023.

[43] Vidar Stiernström, Lukas Lundgren, Murtazo Nazarov, and Ken Mattsson. A residual-based artificial viscosity finite difference method for scalar conservation laws. *Journal of Computational Physics*, 430:110100, 2021.

[44] Michael Stocker. Infrasonic acoustic energy produced by offshore wind turbine energy generation may interfere with bird and cetacean navigation cues. *Environmental Science and Pollution Research*, 33(15):6894–6902, 2026.

[45] Anne Tolvanen, Henri Routavaara, Mika Jokikokko, and Parvez Rana. How far are birds, bats, and terrestrial mammals displaced from onshore wind power development? – a systematic review. *Biological Conservation*, 288:110382, 2023.

[46] Wenjie Wang, Yan Yan, Yongnian Zhao, and Yu Xue. Studies on the experimental measurement of the low-frequency aerodynamic noise of large wind turbines. *Energies*, 17(7), 2024.

[47] Kerstin Persson Waye, Michael Smith, and Mikael Ögren. Hälsopåverkan av lågfrekvent buller inomhus. Technical Report 3, Sahlgrenska Akademin Medicinska Institutionen, 2017.

[48] Markus Weichenberger, Martin Bauer, Robert Kühler, Johannes Hensel, Caroline Garcia Forlim, Albrecht Ihlenfeld, Bernd Ittermann, Jürgen Gallinat, Christian Koch, and Simone Kühn. Altered cortical and subcortical connectivity due to infrasound administered near the hearing threshold - evidence from fmri. *PLOS ONE*, 12(4):1–19, 04 2017.